

# GDF11 Protects against Endothelial Injury and Reduces Atherosclerotic Lesion Formation in Apolipoprotein E-Null Mice

Wen Mei<sup>1</sup>, Guangda Xiang<sup>1</sup>, Yixiang Li<sup>2</sup>, Huan Li<sup>1</sup>, Lingwei Xiang<sup>3</sup>, Junyan Lu<sup>1</sup>, Lin Xiang<sup>1</sup>, Jing Dong<sup>1</sup> and Min Liu<sup>1</sup>

<sup>1</sup>Department of Endocrinology, Wuhan General Hospital of Guangzhou Command, Wuhan, Hubei Province, China; <sup>2</sup>Radiation-Diagnostic/Oncology School of Medicine, Emory University, Atlanta, Georgia, USA; <sup>3</sup>Mathematics and Statistics Department, Georgia State University, Atlanta, Georgia, USA

Growth differentiation factor 11 (GDF11) reduces cardiac hypertrophy, improves cerebral vasculature and enhances neurogenesis in ageing mice. Higher growth differentiation factor 11/8 (GDF11/8) is associated with lower risk of cardiovascular events in humans. Here, we showed that adeno-associated viruses-GDF11 and recombinant GDF11 protein improve endothelial dysfunction, decrease endothelial apoptosis, and reduce inflammation, consequently decrease atherosclerotic plaques area in apolipoprotein E<sup>-/-</sup> mice. Moreover, adeno-associated viruses-GDF11 and recombinant GDF11 stabilize atherosclerotic plaques by selectively decreasing in macrophages and T lymphocytes, while increasing in collagen and vascular smooth muscle cells within plaques. In addition, GDF11 inhibit palmitic acid-induced endothelial apoptosis and ameliorate palmitic acid-induced inflammatory response in RAW264.7 macrophages *in vitro*. Mechanistically, GDF11 activates the TGF- $\beta$ /Smad2/3, AMPK/endothelial nitric oxide synthase (eNOS) while suppresses JNK and NF- $\kappa$ B pathways. In humans, circulating GDF11/8 is positively associated with flow-mediated endothelium-dependent dilation in overweight subjects. We concluded that adeno-associated viruses-GDF11 and recombinant GDF11 protect against endothelial injury and reduce atherosclerosis in apolipoprotein E<sup>-/-</sup> mice, thus may be providing a novel approach to the treatment of atherosclerosis.

Received 11 May 2016; accepted 28 July 2016; advance online publication 11 October 2016. doi:10.1038/mt.2016.160

## INTRODUCTION

Growth differentiation factor 11 (GDF11) belongs to the transforming growth factor  $\beta$  (TGF- $\beta$ ) superfamily.<sup>1</sup> GDF11 exerts its function by interacting with activin type IIA and IIB receptors<sup>2</sup> and type I receptor Alk5 (ref. 3) to induce phosphorylation of Smad2/3. Recent studies showed that GDF11 is a circulating factor that declines with age, and restoring systemic GDF11 levels reverses age-related dysfunction in mouse

heart,<sup>4</sup> skeletal muscle,<sup>5</sup> and brain.<sup>6</sup> However, recent publications from Egerman *et al.* and Smith *et al.* argued that GDF11 inhibits skeletal muscle regeneration and has no effect on cardiac hypertrophy.<sup>7,8</sup> Very importantly, new data demonstrated that circulating growth differentiation factor 11/8 (GDF11/8) levels decrease with age in mice as well as other mammalian species and that increasing GDF11/8 levels with exogenous GDF11 regulates cardiomyocyte size.<sup>9</sup> Furthermore, a human study showed that plasma GDF11 concentrations declined with age in nondiabetic control subjects,<sup>10</sup> and the other two clinical reports revealed that higher GDF11 or GDF11/8 levels from large human cohorts are associated with lower risk of cardiovascular events and death, suggesting the GDF11 pathway as a potential new target to improve adverse cardiovascular outcomes associated with aging.<sup>11,12</sup> Thus, future studies are needed to prove the potential beneficial effects of GDF11 on age-associated cardiovascular diseases.

Atherosclerosis, a chronic inflammatory disease of arterial wall, is an aging-related disease, and aging is one of the main risk factors for atherosclerosis.<sup>13</sup> Atherosclerosis is highly prevalent in older persons having catastrophic consequences in their quality of life and increasing disability and mortality in this population.<sup>14,15</sup> However, the potential role of GDF11 on atherosclerosis has not been investigated.

Adeno-associated viruses (AAV) mediate stable gene expression and are suitable for diseases for which long-term transgene expression is needed.<sup>16</sup> AAV can transduce a wide variety of cell types and transgene expression has been reported at least in the retina, skeletal muscle, vascular smooth muscle, and central nervous system. In this study, we evaluated the potential role of the AAV-mediated GDF11 gene transfer (AAV-GDF11) injected via tail vein and exogenous recombinant GDF11 on atherosclerosis in apolipoprotein E-null (apoE<sup>-/-</sup>) mice. The AAV-GDF11 was first expressed in the liver and subsequent released into the circulation. It was found that AAV-GDF11 and recombinant GDF11 were able to improve endothelial dysfunction, decrease endothelial apoptosis and reduce inflammation activity, consequently decrease atherosclerotic plaques area as well as stabilize atherosclerotic plaques in apoE<sup>-/-</sup> mice.

Correspondence: Guangda Xiang, Department of Endocrinology, Wuhan General Hospital of Guangzhou Command, Wuluo Road 627, Wuhan 430070, Hubei Province, China. E-mail: [Guangda64@hotmail.com](mailto:Guangda64@hotmail.com)

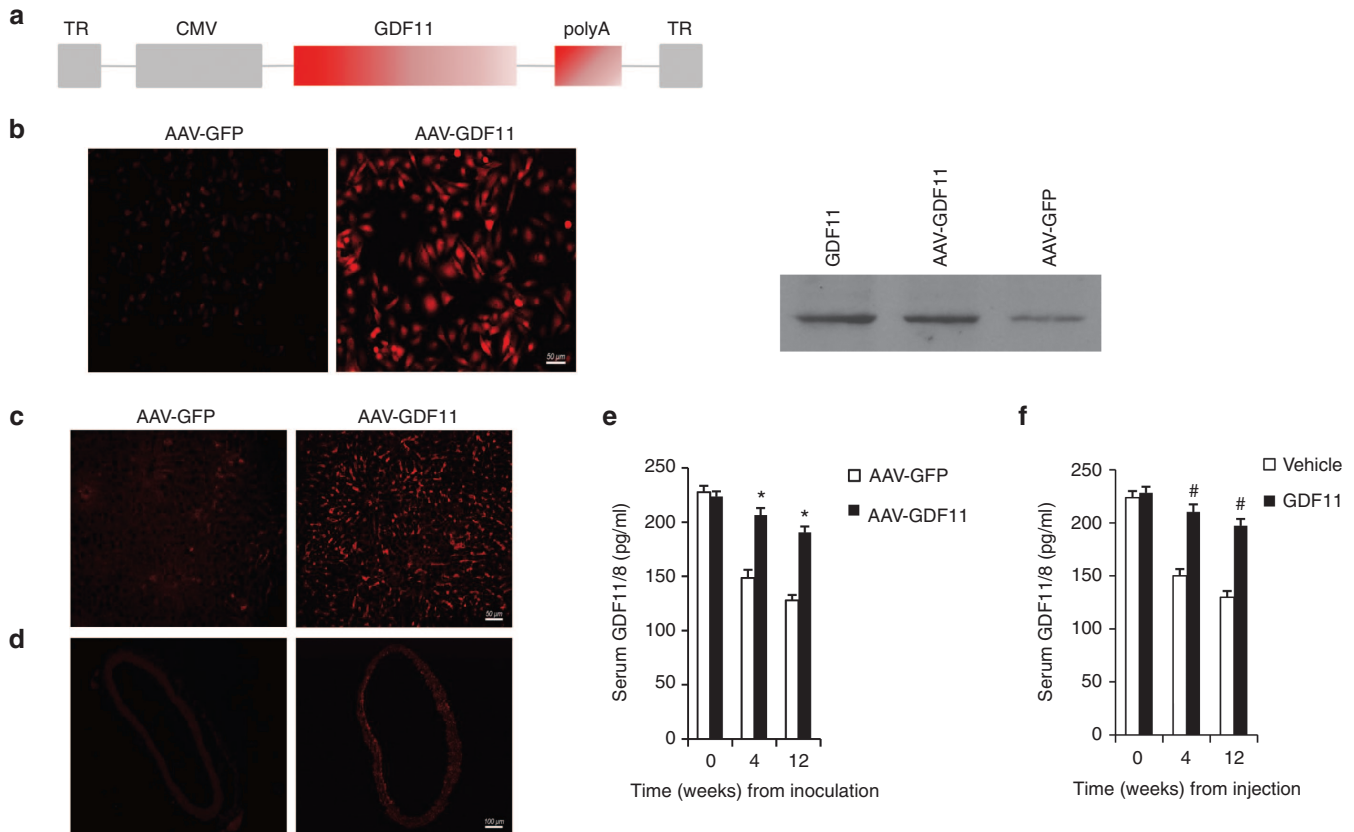


**Figure 1** Delivery of GDF11 cDNA to apoE<sup>-/-</sup> mice using AAV vector. ApoE<sup>-/-</sup> mice ( $n = 13$ ) preinoculated with  $10^{12}$  vp of AAV-GDF11 or AAV-GFP through the tail vein. Randomly three mice from AAV-GFP and AAV-GDF11 groups were killed 4 weeks after injection and the expression of GDF11 in liver and aorta were detected by immunofluorescence. **(a)** AAV vector used in this study. TR indicates terminal repeat sequences; CMV, cytomegalovirus immediate early promoter; and polyA, polyadenylation site. **(b)** Expression of GDF11 was evaluated by immunofluorescence and Western blot in MAECs transduced with AAV-GDF11. Scale bar, 50  $\mu$ m. **(c and d)** All data were repeated three times. Immunofluorescence of liver and aorta sections of mice treated with AAV-GDF11 at 4 weeks after injection. Scale bar, 50  $\mu$ m **(c)** and Scale bar, 100  $\mu$ m **(d)**. **(e and f)** Serum GDF11/8 was analyzed by enzyme-linked immunosorbent assay (ELISA) in apoE<sup>-/-</sup> mice. Data were shown as mean  $\pm$  SD. Student's *t*-test was performed to compare differences between two groups. \* $P < 0.05$  versus AAV-GFP; # $P < 0.05$  versus vehicle group. AAV, adeno-associated viruses; AAV-GDF11, AAV-mediated GDF11 gene transfer; apoE<sup>-/-</sup>, apolipoprotein E null; GDF11, growth differentiation factor 11; GFP, green fluorescent protein; MAECs, mice aortic endothelial cells; SD, standard deviation.

## RESULTS

### Persistence of GDF11 expression in AAV-GDF11 treated apoE<sup>-/-</sup> mice

As an alternative strategy of GDF11 administration, we have constructed an AAV vector-expressing GDF11 (**Figure 1a**) to analyze possible advantages of sustained *in vivo* expression of GDF11 compared with injections with recombinant human GDF11. The AAV-GDF11 vector was used to encapsidate viral particles in serotype 2. Efficiency of transduction and expression of the transgene was initially demonstrated by immunofluorescence and Western blot in cultured mice aortic endothelial cells (MAECs) from apoE<sup>-/-</sup> mice, demonstrating that the transgene is constructed successfully (**Figure 1b**).

In this study, apoE<sup>-/-</sup> mice received a single injection with high-titer ( $\sim 10^{12}$  viral genome particles) AAV-GDF11 or AAV-green fluorescent protein (GFP) through the tail vein. To assess the *in vivo* dissemination of AAV-GDF11, three animals were killed 4 weeks after injection and the expression of GDF11 in liver and aorta were detected by immunofluorescence (**Figure 1c,d**). In both cases, mice injected with AAV-GDF11 showed a large

number of areas positive for expression of GDF11. We also analyzed the serum GDF11/8 levels by enzyme-linked immunosorbent assay and found that GDF11 protein release to the bloodstream remained constant up to 12 weeks (**Figure 1e**) ( $n = 10$  mice in each group).

### The influence of AAV-GDF11 and recombinant GDF11 on metabolic characteristics in animals

Some clinical studies showed that higher circulating GDF11 or GDF11/8 levels are associated with lower risk of cardiovascular events and death.<sup>11,12</sup> It is established that metabolic characteristics are associated with cardiovascular diseases. Thus, we investigated the effects of AAV-GDF11 and recombinant GDF11 on metabolic profiles *in vivo*. Firstly, compared with the normal chow control group, the high fat diet (HFD) control group had higher levels of body weight, serum free fatty acids (FFA) at 0, 4, 8, and 12 weeks, and lower levels of GDF11/8 at 4, 8, and 12 weeks (see **Supplementary Figure S1b–d**). Secondly, to investigate the changes of circulating GDF11/8 levels with age in mice fed with HFD, the results showed that circulating GDF11/8 levels have a trend of decrease

at 0 week when compared with -8 weeks ( $P > 0.05$ ), which significantly lower at 4, 8, and 12 weeks as compared with -8 weeks and 0 week ( $P < 0.05$ ) (see **Supplementary Figure S1d**). Thirdly, to explore the changes of circulating GDF11/8 in mice induced by different interventions, serum GDF11/8 levels were measured at 0 week ( $n = 13$  mice in each group), 4 weeks ( $n = 3$  mice in each group), and 12 week time point ( $n = 10$  mice in each group). Serum GDF11/8 levels declined with age in the AAV-GFP and vehicle groups ( $P < 0.05$ ) and were significantly elevated in the AAV-GDF11 and recombinant GDF11 groups at 4 and 12 weeks time points ( $P < 0.05$ ) (**Figure 1e,f**). Fourthly, body weight, systolic blood pressure, and other metabolic parameters were analyzed at different experiment time points. The body weight increased dramatically from -8 weeks ( $17.3 \pm 0.7$  g,  $n = 102$  mice) to 0 weeks ( $23.4 \pm 1.9$  g,  $n = 92$  mice) ( $P < 0.01$ ) in intervention apoE<sup>-/-</sup> mice. The body weight and systolic blood pressure levels were not statistically different among AAV-GFP, AAV-GDF11, vehicle and GDF11-treated groups at 0 and 12 weeks (see **Supplementary Table S1**). After different treatments for 12 weeks, as shown in **Supplementary Table S2**, AAV-GDF11 and GDF11 had no significant effects on fasting glucose, glycosylated hemoglobin (HbA1c) and high density lipoprotein. However, the serum levels of fasting insulin, interleukin-6 (IL-6), tumor necrosis factor- $\alpha$  (TNF- $\alpha$ ), c-reactive protein, oxidized low density lipoprotein, total cholesterol, triglycerides and FFA were significantly decreased at the end of this study in AAV-GDF11 and GDF11 groups when compared with the AAV-GFP or vehicle groups. Fifthly, to test the effects of AAV-GDF11 and recombinant GDF11 on insulin sensitivity in mice fed with HFD, intraperitoneal glucose tolerance test and insulin tolerance test were performed before and 12 weeks after AAV-GDF11 or others treatments. Before these interventions, there was no significant difference on glucose and insulin tolerance among the four groups. But after 12 weeks of interventions, the glucose and insulin tolerance were improved significantly when compared with the AAV-GFP or vehicle groups (see **Supplementary Figures S2 and S3**).

### AAV-GDF11 and recombinant GDF11 protected against endothelial injury *in vivo*

Previous study revealed that GDF11 treatment induces migration and *in vitro* tube formation of peripheral blood endothelial progenitor cells.<sup>17</sup> Thus, the effects of AAV-GDF11 and recombinant GDF11 on endothelial injury *in vivo* were detected in this study. Firstly, the protective roles of AAV-GDF11 and GDF11 on endothelial function *in vivo* were measured at 4 weeks. Both AAV-GDF11 and GDF11 treatments improved the vascular endothelium-dependent relaxation in response to acetylcholine when compared with the AAV-GFP or vehicle groups ( $71.32 \pm 3.89\%$  versus  $87.17 \pm 4.13\%$ ;  $73.61 \pm 3.63\%$  versus  $89.83 \pm 3.52\%$  relaxation at  $10^{-4}$  mmol/l acetylcholine, respectively; four aortic rings from each mice,  $n = 3$  mice in each group,  $P < 0.05$ ) (**Figure 2a**). In contrast, the vascular endothelium-independent relaxation in response to sodium nitroprusside did not differ among the 4 groups (**Figure 2b**). Secondly, apoptosis of endothelial cells has been suggested to play a unfavorable role in atherosclerosis.<sup>18</sup> Thus, the effects of AAV-GDF11 and recombinant GDF11 on the apoptosis of endothelial cell *in vivo* were explored at 12 weeks. The serial

plaque sections from the thoracic aorta were costained for terminal deoxynucleotidyl transferase biotin-dUTP nick end labeling and CD31, an endothelial cell-specific marker. As shown in **Figure 2c,d**, both AAV-GDF11 and GDF11 treatments had sparse terminal deoxynucleotidyl transferase-mediated dUTP-biotin nick end labeling -positive cells that seldom colocalized with endothelial cells compared with the AAV-GFP or vehicle treatments. It means that a greater more integrity of endothelial cells laid on the plaque surface of AAV-GDF11 and GDF11-treated mice. In addition, electron microscopy of arterial endothelium revealed arteries from the AAV-GFP and vehicle groups had extensive endothelial damage characterized by nuclear condensation and cytoplasmic vacuolization, while most arterial endothelium from the AAV-GDF11 and GDF11 groups was intact (**Figure 2e**). These findings suggest that AAV-GDF11 and recombinant GDF11 decreased endothelial injury in apoE<sup>-/-</sup> mice fed a HFD.

### AAV-GDF11 and recombinant GDF11 attenuated atherosclerotic lesion formation in apoE<sup>-/-</sup> mice

Endothelial injury is the early pathophysiologic change of atherosclerosis, approaches that protect against endothelial injury may be therapeutic for atherosclerosis.<sup>19</sup> Therefore, we investigated whether AAV-GDF11 and recombinant GDF11 alleviate atherosclerosis besides protecting vascular endothelium at 12 weeks in this study. Firstly, the lipid-rich atherosclerotic lesion area, including both en face and cross sections analyses, was significantly smaller in the AAV-GDF11 group compared with the AAV-GFP group (en face:  $14.54 \pm 2.86\%$  versus  $38.01 \pm 4.43\%$ , cross sections:  $9.06 \pm 1.63\%$  versus  $23.02 \pm 2.76\%$ ,  $P < 0.05$ ) (**Figure 3a,c**). Similarly, the recombinant GDF11 significantly decreased the plaque area compared with the vehicle group (en face:  $17.18 \pm 2.17\%$  versus  $31.23 \pm 3.12\%$ , cross sections:  $10.32 \pm 1.47\%$  versus  $19.87 \pm 2.11\%$ ,  $P < 0.05$ ) (**Figure 3a,c**). Secondly, we sought to investigate whether, besides decreasing the development of atherosclerotic lesions, AAV-GDF11 and recombinant GDF11 treatment also affected their cellular composition. For this purpose, serial plaque sections from the aortic arch were analyzed by immunohistochemistry to quantitatively evaluate the vascular smooth muscle cells (VSMCs), collagen content, macrophages, T lymphocytes, matrix metalloproteinase (MMP)-2 and MMP-9. As shown in **Figure 3e,f**, the relative contents of VSMCs and collagen were higher in the AAV-GDF11 and GDF11 groups, possibly contributing to the stability of atherosclerotic plaques. In contrast, AAV-GDF11 and GDF11 treatments significantly reduced the area of macrophages and T lymphocytes infiltration in plaques compared with the AAV-GFP or vehicle groups (**Figure 3e,f**). Furthermore, the expression levels of MMP-2 and MMP-9 were lower in the AAV-GDF11 and GDF11 groups (see **Supplementary Figure S4**). These findings appear particularly relevant because plaque infiltrating macrophages are through production of metalloproteinases to induce plaque destabilization.<sup>20</sup>

It is established that atherosclerosis is an inflammatory disease of arterial wall.<sup>21</sup> Next, we assessed the inflammatory cytokines in aortas by real-time polymerase chain reaction. As shown in **Figure 3g**, GDF11 treatment dramatically reduced the mRNA expression levels of IL-6, IL-1 $\beta$ , TNF- $\alpha$ , monocyte chemoattractant

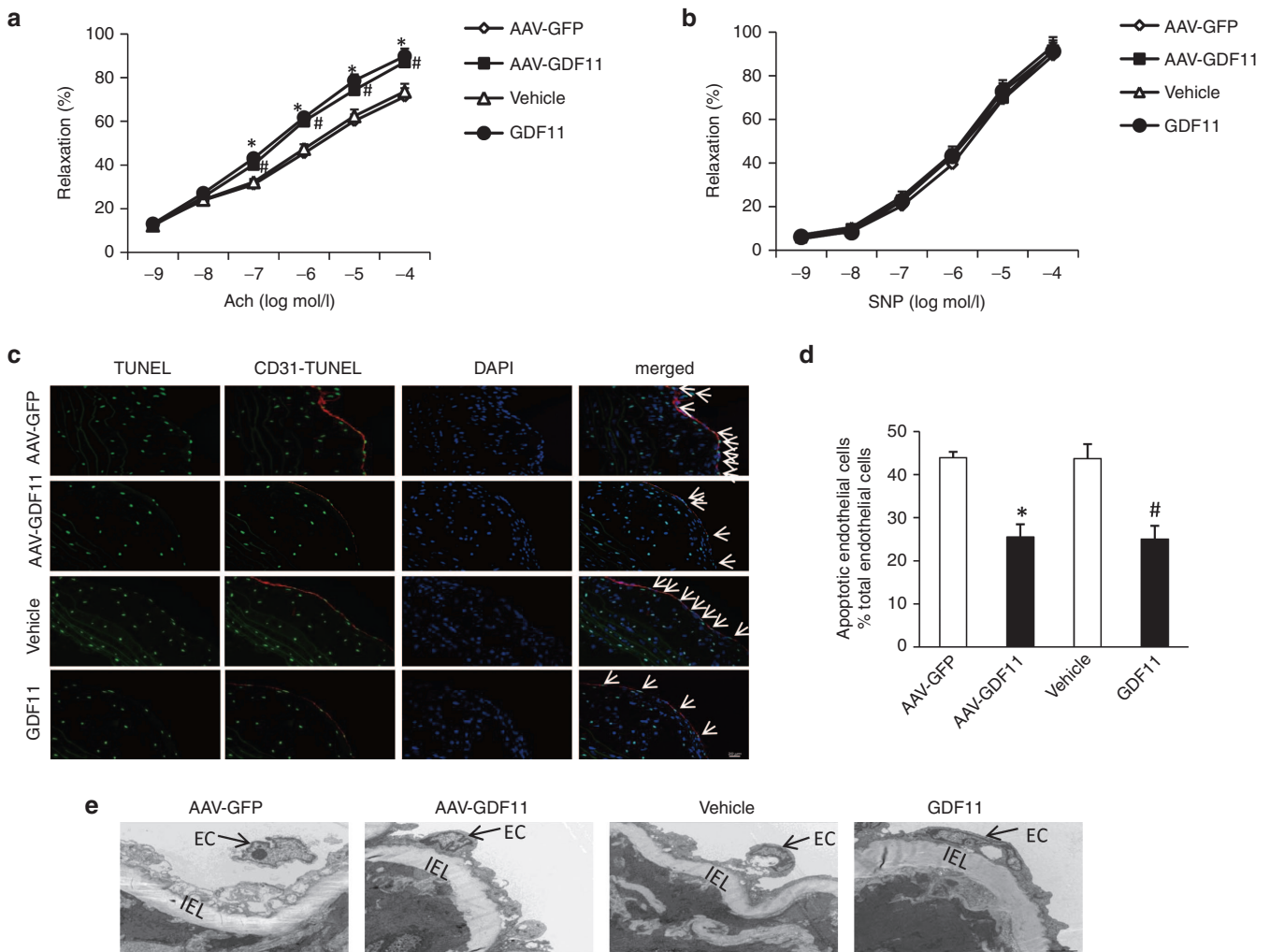


**Figure 2** AAV-GDF11 and GDF11 improved endothelial function and decreased endothelial cells apoptosis in apoE<sup>-/-</sup> mice. Four thoracic aorta rings from each apoE<sup>-/-</sup> mice (*n* = 3 mice from each group) were equilibrated for 1 hour at a preload tension of 0.5 g in Krebs buffer and then precontracted with norepinephrine (NE, 10<sup>-6</sup> mmol/l). Once a steady state was achieved, vasodilation responses were evaluated by cumulative concentration-response curves to (a) acetylcholine (ACh, 10<sup>-9</sup>–10<sup>-4</sup> mmol/l) and (b) sodium nitroprusside (SNP, 10<sup>-9</sup>–10<sup>-4</sup> mmol/l). (c) Five continuous sections from each apoE<sup>-/-</sup> mice (*n* = 4 mice from each group) were costained with terminal deoxynucleotidyl transferase-mediated dUTP-biotin nick end labeling (TUNEL) (apoptotic cells, green), anti-CD31 (endothelial cells, red) and 4',6-diamidino-2-phenylindole (DAPI) (nuclei; blue). (d) The percentage of apoptotic endothelial cells per total endothelial cells. (e) Electron microscopy was performed on thoracic aortas using ultrathin sections and examined with a Nikon EclipseE800 light microscope. Arrow shows endothelial cell (EC), IEL: internal elastic lamina. Scale bar, 20 μm. Data were shown as mean ± SD. Differences between 2 groups were tested with Student's *t*-test. \**P* < 0.05 versus AAV-GFP; #*P* < 0.05 versus vehicle group. AAV, adeno-associated viruses; AAV-GDF11, AAV-mediated GDF11 gene transfer; apoE<sup>-/-</sup>, apolipoprotein E null; GDF11, growth differentiation factor 11; GFP, green fluorescent protein; SD, standard deviation.

peptide-1 (MCP-1), interferon (IFN)-γ, but increased the levels of IL-10 in aortas (*P* < 0.05).

**GDF11 induced the proliferation and inhibited palmitic acid-induced apoptosis of endothelial cells *in vitro***

As is known, high-fat diets are commonly used in rodents to induce obesity, increase serum FFA and induce lipotoxicity in various organs. High levels of circulating FFA are able to induce inflammation effect and impair endothelial function.<sup>22</sup> Our animal results also showed that serum FFA increased significantly in control group fed with HFD compared with normal chow. Therefore, PA was used to treat cells in the *in vitro* experiments.

As shown in above, AAV-GDF11 and GDF11 can protect against endothelial injury in mice fed with HFD. Next, we questioned whether endothelial cells can benefit from GDF11 treatment *in vitro*. Firstly, the proliferation of MAECs measured by EdU-kit did not differ among the vehicle, GDF11 and GDF11 + SB431542 (10 μmol/l, a TβR1-Smad2/3 inhibitor) groups at 1-day and 3-day time points (Data not shown). However, a 5-day treatment of MAECs with GDF11 increased their proliferation by 37.12% as compared with that of vehicle, but not in the presence of GDF11 + SB431542 (see **Supplementary Figure S5a,b**). Secondly, With regard to the effect of GDF11 on the migration of MAECs and macrophages, no significant differences were found in the cell numbers among the vehicle, GDF11 and GDF11 + SB431542 groups (see **Supplementary Figure S5c-e**).

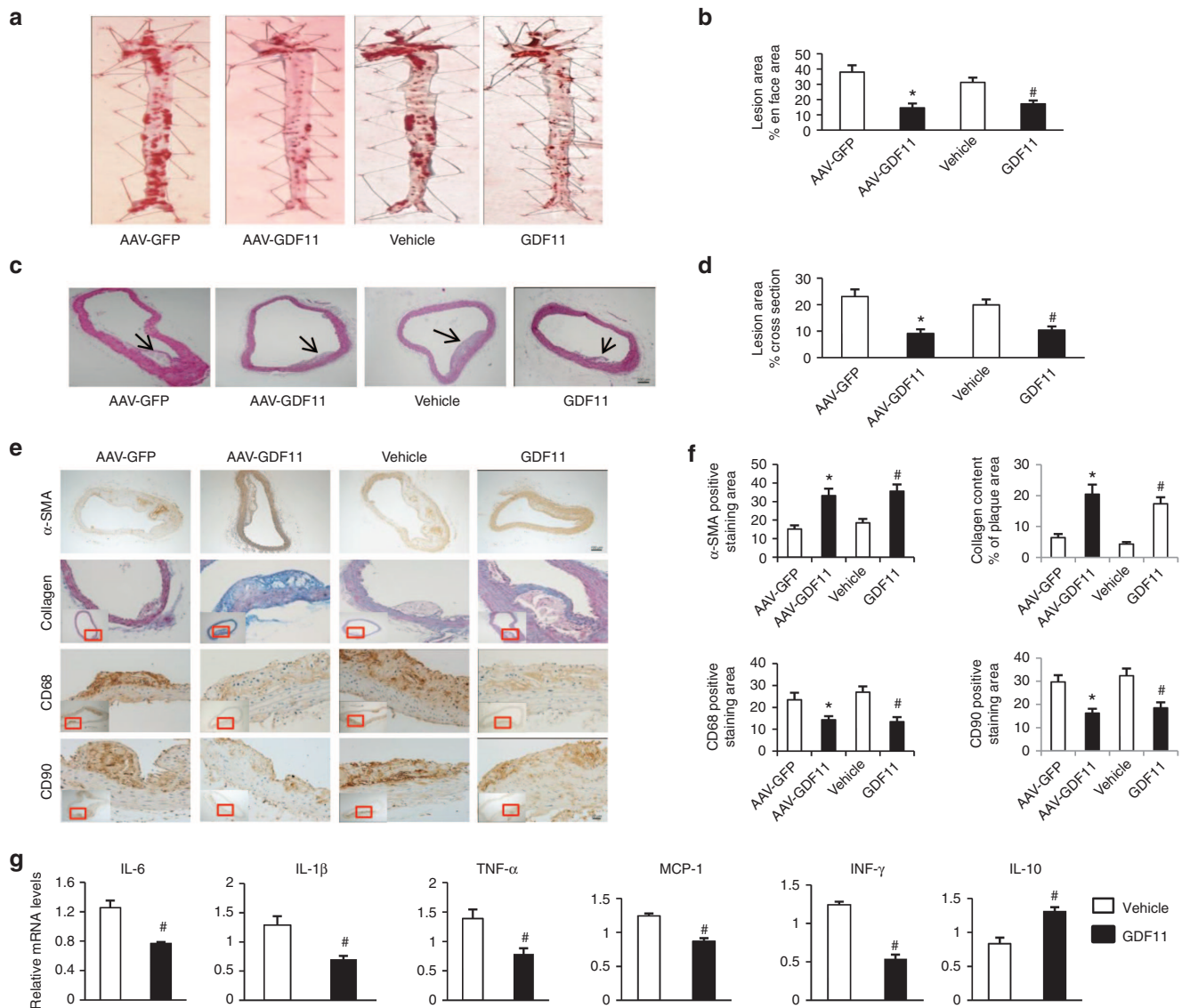


**Figure 3** AAV-GDF11 and GDF11 attenuated atherosclerotic lesion formation, ameliorated plaque components and inflammatory cytokines in aortas of apoE<sup>-/-</sup> mice. **(a)** Oil red O staining of the whole aorta ( $n = 4$  mice in each group) was performed to analyze the en face atherosclerotic lesions area. **(b)** Quantitative analysis of **a**. **(c)** Hematoxylin and eosin staining ( $n = 4$  mice in each group) was performed to quantify luminal cross-sectional area involved by atherosclerotic plaque. **(d)** Quantitative analysis of **c**. **(e)** Immunohistochemical staining of  $\alpha$ -SMA, anti-CD68, and anti-CD90 were performed to analyze the VSMCs, macrophages and T lymphocytes expression levels. Scale bar, 20  $\mu$ m. Masson's trichrome staining was performed to quantification of collagen content. Scale bar, 100  $\mu$ m. **(f)** Quantitative analysis of **e**. **(g)** mRNA expression levels of IL-6, IL-1 $\beta$ , TNF- $\alpha$ , MCP-1, IFN- $\gamma$ , and IL-10 measured by quantitative real-time polymerase chain reaction (PCR) in the abdominal aorta ( $n = 6$  mice in each group) and expressed relative to  $\beta$ -actin. Data were shown as mean  $\pm$  SD. Differences between two groups were tested with Student's  $t$ -test. \* $P < 0.05$  versus AAV-GFP; # $P < 0.05$  versus vehicle group. AAV, adeno-associated viruses; AAV-GDF11, AAV-mediated GDF11 gene transfer; apoE<sup>-/-</sup>, apolipoprotein E null; GDF11, growth differentiation factor 11; GFP, green fluorescent protein; TNF- $\alpha$ , tumor necrosis factor- $\alpha$ ; IL, interleukin; IFN- $\gamma$ , interferon- $\gamma$ ; VSMCs, vascular smooth muscle cells; SD, standard deviation.

Before the next experiment, we explored the time- and dose-dependent of PA-induced viability by MTT. As shown in **Supplementary Figure S6a**, we chose PA 0.4 mmol/l and 24 hours as the optimum concentration and time condition in the following study. Compared with the vehicle group, the percentage of apoptotic MAECs in PA group was significantly increased, and the effect was blocked by cotreatment with GDF11 (**Figure 4a,b**). Consistent with these findings, we also found that GDF11 significantly decreased the apoptotic proteins (cleaved-caspase-3 and bax) expression and increased the

antiapoptotic protein (bcl-2) expression in PA treated MAECs (**Figure 4c,d**).

### GDF11 reduced PA-induced inflammatory cytokines expression in RAW264.7 macrophages

It has been shown that macrophages represent a key cellular component of innate immunity, which has been shown to promote atherosclerosis initiation and progression.<sup>23</sup> Previous study showed that HFD significantly induced the mRNA expression of inflammatory factors in peritoneal macrophages in

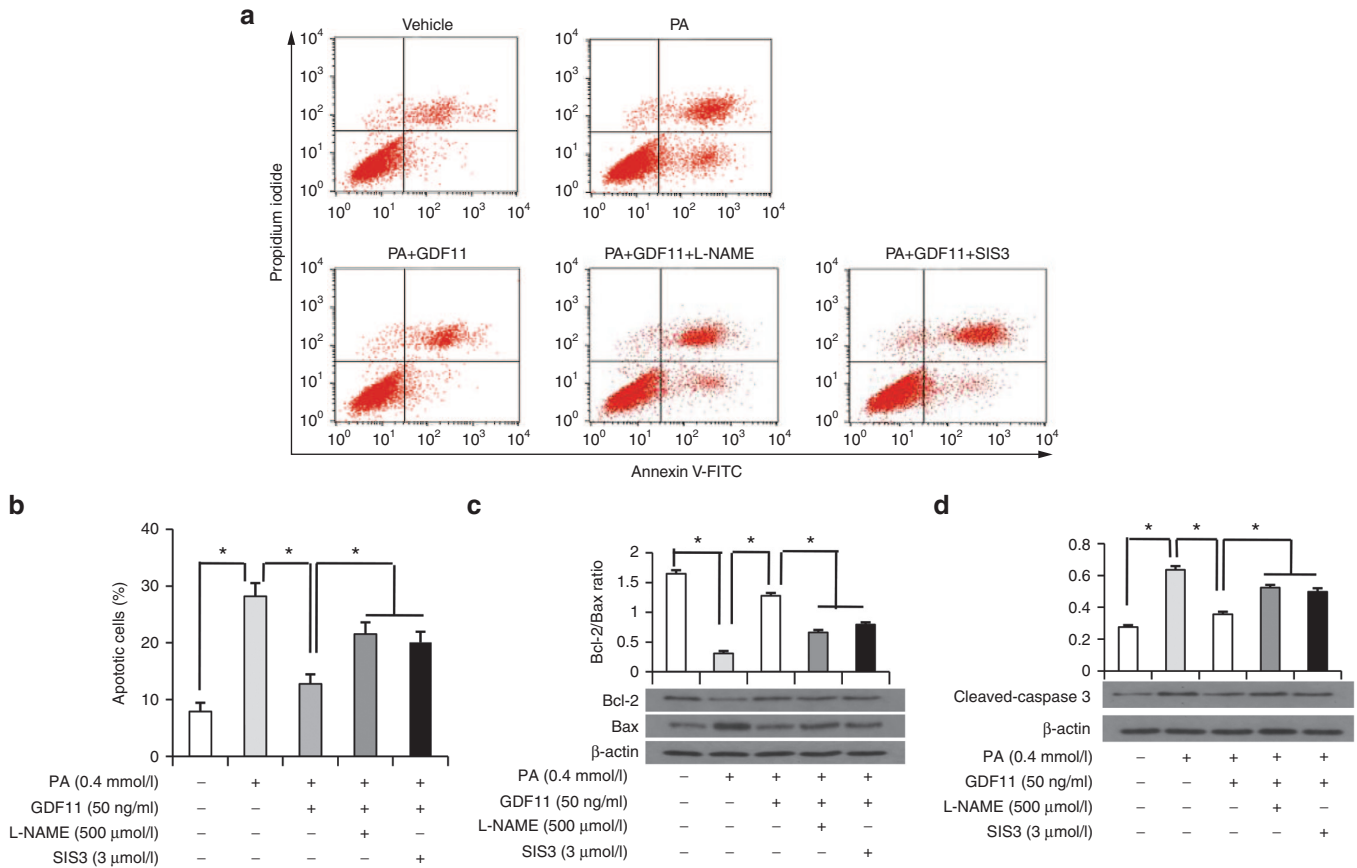


**Figure 4** GDF11 reduced the palmitic acid-induced apoptosis of MAECs. **(a)** Representative images of apoptotic cells stained with annexin-V-FITC and propidium iodide in MAECs pretreated with or without L-NAME (500 μmol/l) or SIS3 (3 μmol/l) for 30 minutes before treatment with GDF11 (50 ng/ml) for 30 minutes, then treated with PA (0.4 mmol/l) or vehicle for 24 hours. **(b)** The percentage of apoptotic cells. **(c and d)** Expression of Bcl-2, Bax, and cleaved-caspase 3 in MAECs were determined by western blot with the above treatments in comparison to β-actin. Data were shown as mean ± SD. Analysis of variance (ANOVA) followed by LSD *t*-test was used to compare the differences among different groups. Each experiment repeated five times. \**P* < 0.05. GDF11, growth differentiation factor 11; MAECs, mice aortic endothelial cells; SD, standard deviation; LSD, least significant difference.

apoE<sup>-/-</sup> mice.<sup>24</sup> Therefore, next we questioned whether GDF11 ameliorated PA-induced inflammatory cytokines expression levels of IL-6, TNF-α, MCP-1, and IL-10 in RAW264.7 macrophages. Similarly, we explored the time- and dose-dependent responses of PA-induced inflammation (evaluated by IL-6 and TNF-α production) by enzyme-linked immunosorbent assay. As shown in **Supplementary Figure S6b,c**, we chose PA 0.4 mmol/l and 16 hours as the optimum concentration and time condition for macrophages incubation in the following study. After stimulating 16 hours, GDF11 significantly attenuated PA-induced inflammation response (IL-6, TNF-α, MCP-1, and IL-10). However, Pretreatment with SB431542 significantly attenuated the inhibitory effects of GDF11 on PA-induced inflammatory response (see **Supplementary Figure S7**).

**The possible signaling mechanisms of protective effects of GDF11 on atherosclerosis *in vivo* and *in vitro***

In the last experiments, we explored the possible signaling mechanisms of protective effects of GDF11 on atherosclerosis *in vivo* and *in vitro*. Firstly as one member of the TGF-β superfamily, GDF11 binds to specific receptors with serine-threonine kinase activity, leading to intracellular signaling through the activation

of the canonical pathway Smad 2/3. To explore whether Smad 2/3 is involved in the protective effects of AAV-GDF11 and GDF11 on artery in our study, proteins extracted from aortas were analyzed by Western blot. As shown in **Figure 5a,b**, both AAV-GDF11 and GDF11 treatments significantly increased Smad2/3 phosphorylation cascade (*P* < 0.05). In the *in vitro* experiments, treating MAECs and RAW264.7 cells with GDF11 (50 ng/ml) activated the canonical TGF-β/Smad signaling pathway, revealed by an increase in the Smad2/3 phosphorylation cascade, whereas this effect could be blocked by coincubation with SB431542 (**Figure 5c-f**). Secondly, we explored the noncanonical signaling pathway of GDF11 in our study. In the *in vivo* experiment, proteins extracted from thoracic aortas after 12 weeks of GDF11 or others treatments were analyzed by Western blot, and the results showed that AAV-GDF11 and GDF11 treatments significantly increased eNOS phosphorylation when compared with the AAV-GFP or vehicle groups (**Figure 6a,b**). Nitric oxide (NO), produced by eNOS, plays a pivotal role in regulating endothelial cell function, apoptosis, and exhibits athero-protective effects.<sup>25,26</sup> Accordingly, AAV-GDF11 and GDF11 treatments significantly increased the NO levels compared with the AAV-GFP or vehicle groups (see **Supplementary Figure S8a**), which are consistent

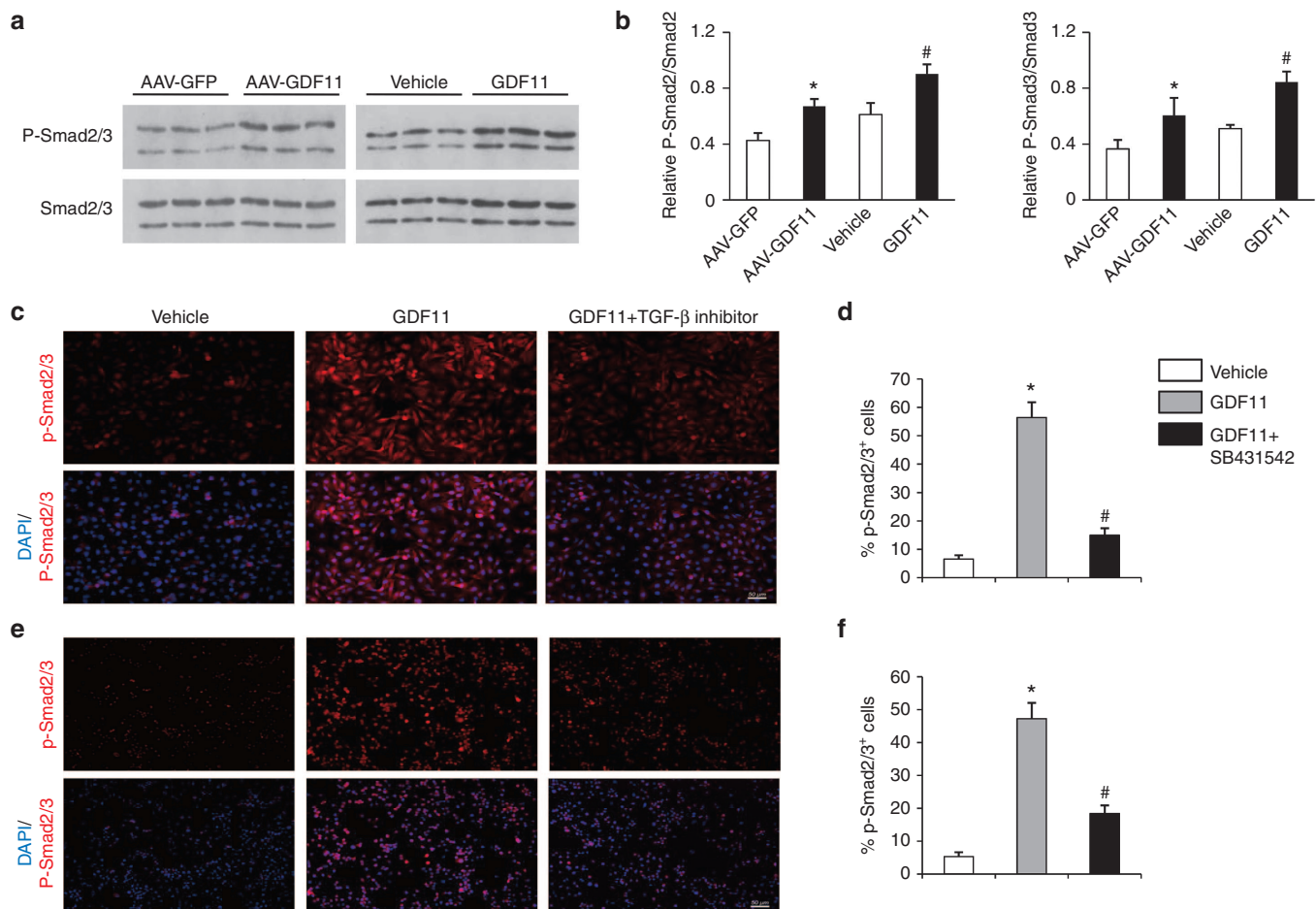


**Figure 5** GDF11 activated TGF- $\beta$ /Smad pathways *in vivo* and *in vitro*. **(a)** Expression of Smad2/3 and phosphorylated Smad2/3 in the aortas of apoE<sup>-/-</sup> mice were determined by western blot 12 weeks post GDF11 or others treatments. **(b)** Quantitative analysis of **a**. Data were shown as mean  $\pm$  SD. Differences between two groups were tested with Student's *t*-test.  $n = 3$  mice in each group. \* $P < 0.05$  versus AAV-GFP; # $P < 0.05$  versus vehicle group. **(c and e)** Representative images of the percentage of phosphorylated-Smad2/3<sup>+</sup> cells in **c** MAECs and **e** RAW 264.7 macrophages treated with either GDF11 (50 ng/ml) for 30 minutes or pretreated with SB431542 (10  $\mu$ mol/l) for 30 minutes, and then treated with GDF11 (50 ng/ml) for 30 minutes. **(d and f)** Quantitative analysis of **c** and **e**. Data were shown as mean  $\pm$  SD. Analysis of variance (ANOVA) followed by LSD *t*-test was used to compare the differences among different groups. Each experiment repeated five times. \* $P < 0.05$  versus vehicle; # $P < 0.05$  versus GDF11 group. AAV, adeno-associated viruses; AAV-GFP, AAV-green fluorescent protein; GDF11, growth differentiation factor 11; MAECs, mice aortic endothelial cells; SD, standard deviation; TGF- $\beta$ , transforming growth factor; LSD, least significant difference.

with eNOS phosphorylation levels in aortas of four groups. The phosphorylation of eNOS can be regulated by several kinases.<sup>27</sup> Thus, we examined the changes in the levels of cAMP-dependent protein kinase (PKA), adenosine monophosphate-activated protein kinase (AMPK) and Akt/protein kinase B in aortas. AAV-GDF11 and GDF11 treatments for 12 weeks increased AMPK phosphorylation when compared with the AAV-GFP or vehicle groups, but did not influence the protein expression of PKA and Akt (**Figure 6a,b**). We next verified this noncanonical signaling pathway in cultured MAECs. First of all, the time-course of phosphorylated endothelial nitric oxide synthase (P-eNOS) expression *in vitro* showed that GDF11 activated P-eNOS expression after 15 minutes treatment (50 ng/ml), reached the highest P-eNOS expression after 30 minutes, reduced P-eNOS expression after 36 hours treatment (see **Supplementary Figure S9a**). Secondly, we found incubation of MAECs with 50 ng/ml GDF11 for 30 minutes increased AMPK and eNOS phosphorylation. However, the activatory effects of GDF11 on AMPK and

eNOS phosphorylation were blocked Compound C (an AMPK inhibitor) or L-NAME (an eNOS inhibitor) (see **Supplementary Figure S9b,c**). As expected, the expressions of PKA and Akt did not differ among different treatment groups (see **Supplementary Figure S9d,e**). These findings indicate that GDF11 could activate AMPK/eNOS signaling pathway. Next, we measured the production of NO in culture media and found GDF11 significantly increased NO synthesis. However, the GDF11-induced increase in NO production was attenuated in the presence of Compound C or L-NAME (see **Supplementary Figure S8b**). More importantly, pretreatment MAECs with L-NAME or SIS3 (a Smad3 inhibitor), significantly attenuated the inhibitory effects of GDF11 on PA-induced endothelial apoptosis (**Figure 4a,b**). This suggested that the antiapoptotic effect of GDF11 on MAECs may through the TGF- $\beta$ /Smad and AMPK/eNOS pathways. Thirdly, pretreatment with GDF11 significantly inhibited PA-induced phosphorylation of c-jun N-terminal kinase (JNK) and nuclear factor-kappa B (NF- $\kappa$ B) p65 nuclear translocation, but had no

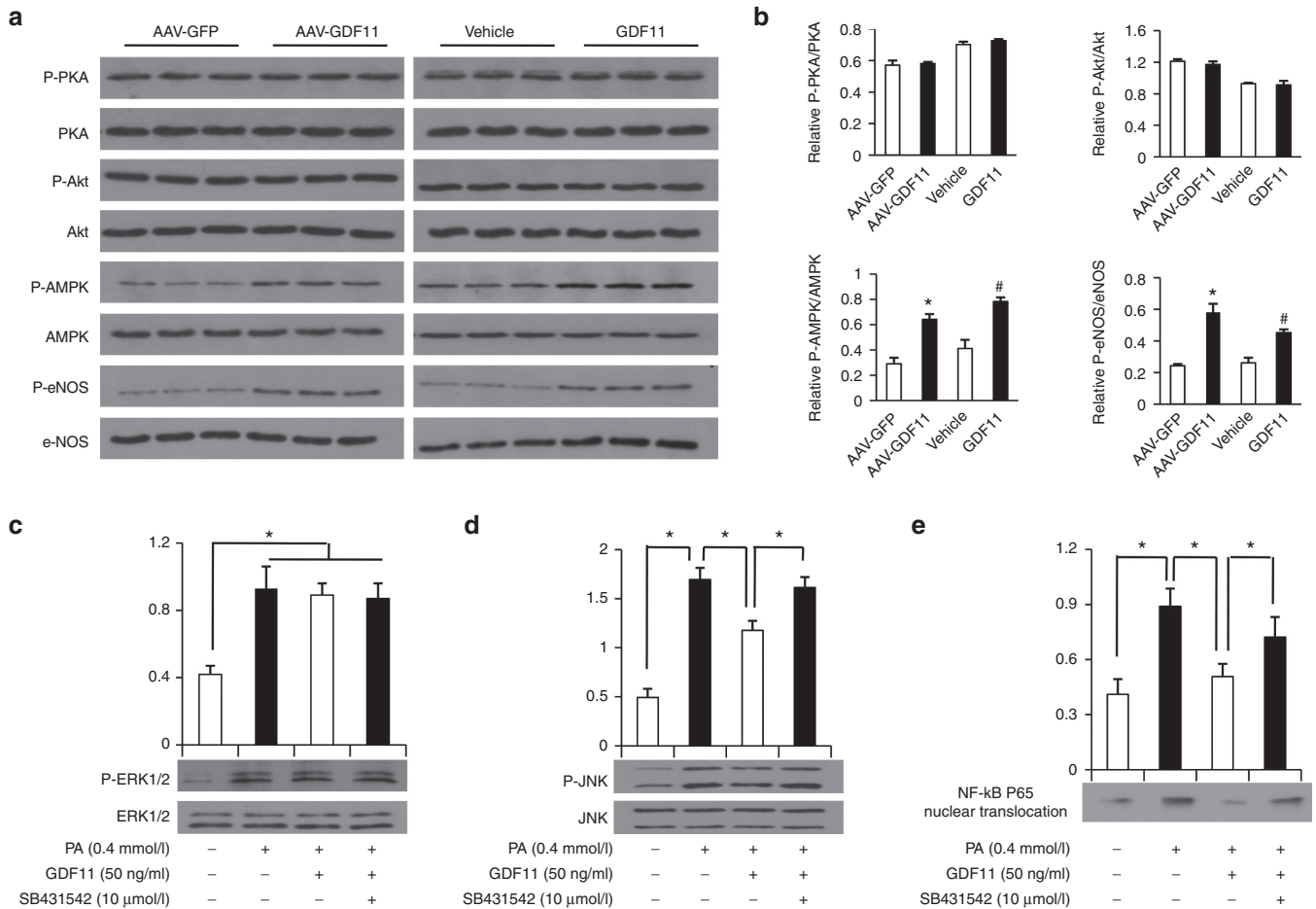


**Figure 6** GDF11 activated AMPK/eNOS signaling *in vivo* and inhibited inflammation signaling pathways in RAW264.7 macrophages. **(a)** Expression of PKA, P-PKA, Akt, P-Akt, AMPK, P-AMPK, eNOS, and P-eNOS in the aortas of apoE<sup>-/-</sup> mice were determined by western blot 12 weeks post AAV-GDF11 or others treatments. **(b)** Quantitative analysis of **(a)**. Data were shown as mean ± SD. Differences between two groups were tested with Student's *t*-test. *n* = 3 mice in each group. \**P* < 0.05 versus AAV-GFP; #*P* < 0.05 versus vehicle group. **(c-e)** Expression of ERK1/2, P-ERK1/2, JNK, P-JNK, and NF-κB P65 nuclear translocation levels in RAW264.7 macrophages were determined by western blot. Cells were pretreated with SB431542 for 30 minutes, and then treated with GDF11 (50 ng/ml) for 1 hour followed by stimulation with PA (0.4 mmol/l). Data were shown as mean ± SD. Analysis of variance (ANOVA) followed by LSD *t*-test was used to compare the differences among different groups. Each experiment repeated five times. \**P* < 0.05. AAV, adeno-associated viruses; AAV-GFP, AAV-green fluorescent protein; GDF11, growth differentiation factor 11; SD, standard deviation; AMPK, adenosine monophosphate-activated protein kinase; P-eNOS, phosphorylated endothelial nitricoxide synthase; ERK1/2, extracellular signal-regulated kinase1/2; JNK, c-jun N-terminal kinase; NF-κB, nuclear factor-kappa B; LSD, least significant difference; PA, palmitic acid.

effect on PA-induced phosphorylation of extracellular signal-regulated kinase1/2 (ERK1/2) in RAW264.7 macrophages. The addition of SB431542 significantly attenuated the inhibitory effects of GDF11 on PA-induced phosphorylation of JNK and NF-κB p65 activation (**Figure 6c-e**). These results indicate that GDF11 could reduce inflammatory cytokines in macrophages via inhibition of intracellular inflammatory signaling, including JNK and NF-κB p65.

**Human studies**

**Circulating GDF11/8 is positively related with endothelium-dependent vasodilation in overweight subjects.** The clinical characteristics and biochemical data of the control and overweight subjects were summarized in online **Supplementary Information** (see **Supplementary Table S3**). Compared with the control subjects, circulating GDF11/8 levels were significantly lower (*P* = 0.002) in overweight subjects. By dividing the distribu-

tion of flow-mediated endothelium-dependent artery dilatation (FMD) in overweight subjects, compared with subjects in the lowest quartile of FMD levels, those in the highest had significantly higher GDF11/8 concentrations (*P* for trend < 0.001) (see **Supplementary Table S4**). Moreover, the GDF11/8 levels in the quartile 3 and quartile 4 were significantly higher as compared with those in the quartile 1 after adjustment for age and body mass index (**Figure 7a**). Multiple stepwise regression analysis showed that GDF11/8, age, body mass index, low density lipoprotein cholesterol, FFA, c-reactive protein, homeostasis model assessment of insulin resistance and fasting insulin were found to be independently associated with FMD levels (all *P* < 0.05) (see **Supplementary Table S5**). The correlation analysis showed that circulating GDF11/8 levels were associated with FMD levels (*r* = 0.452, *P* < 0.001) (**Figure 7b**). In addition, circulating GDF11/8 concentrations declined with age (**Figure 7c**) (*P* < 0.01 for trend). By logistic regression analysis the odds ratio for lower



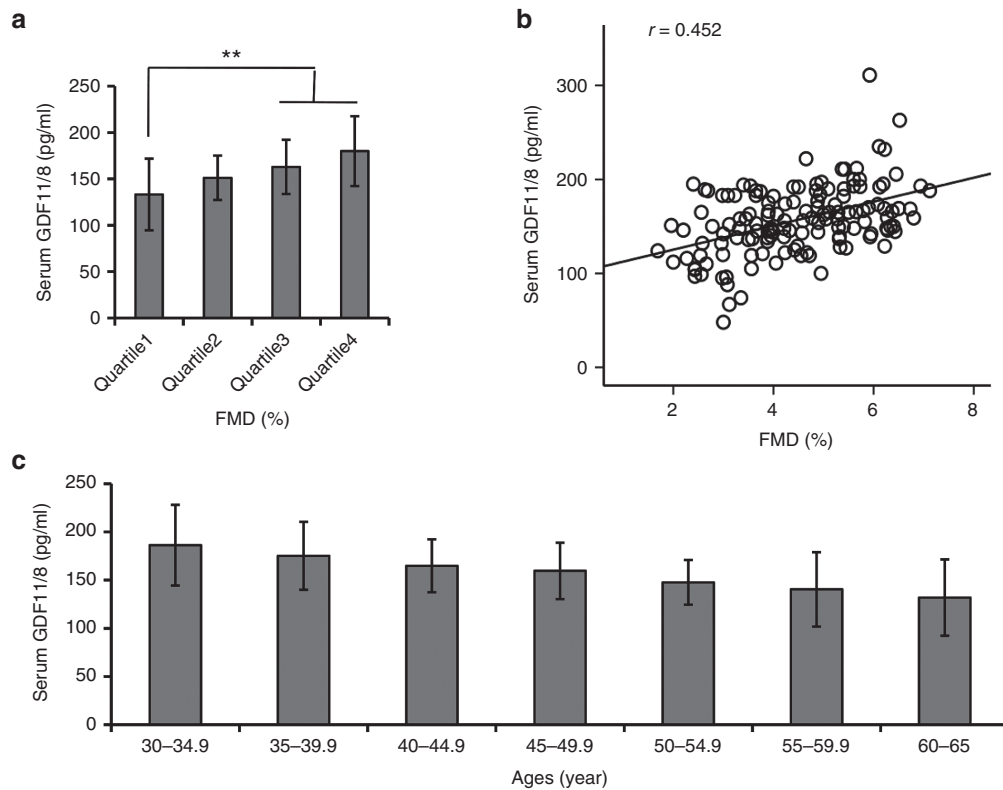


**Figure 7** Circulating GDF11/8 is positively related with endothelium-dependent vasodilation in overweight subjects. **(a)** Circulating GDF11/8 concentrations in different quartiles of FMD levels in overweight subjects. Data were shown as mean  $\pm$  SD. Analysis of variance (ANOVA) followed by LSD *t*-test was used to compare the differences among different groups.  $**P < 0.01$  versus Quartile 1. **(b)** Correlation analysis to evaluate correlation of circulating GDF11/8 with FMD in overweight subjects. Correlation was performed using Pearson's method. **(c)** The changes of plasma GDF11/8 with ages in this study group. The GDF11/8 levels declined with age ( $P < 0.01$  for trend). ANOVA followed by LSD *t*-test was used to compare the differences among different groups. GDF11, growth differentiation factor 11; SD, standard deviation; FMD, flow-mediated endothelium-dependent artery dilatation; LSD, least significant difference.

FMD levels was reduced by 14.4% per 1 pg/ml increase in the GDF11/8 concentration (OR (95% CI); 0.856 (0.647–0.984)) (see **Supplementary Table S6**).

## DISCUSSION

The major finding of this study was that (i) AAV-GDF11 and exogenous recombinant GDF11 improved endothelial injury and reduced atherosclerosis lesion formation in apoE<sup>-/-</sup> mice fed a HFD; (ii) AAV-GDF11 and exogenous recombinant GDF11 enhanced mature plaque stability via increasing VSMCs and collagen content and reducing macrophages, MMPs activities and inflammatory cytokine expression; (iii) the molecular mechanisms underlying these beneficial effects may involve the activation of the canonical Smad2/3 pathway and the noncanonical signaling pathways including activation of AMPK/eNOS and inhibition of inflammation pathways; and (iv) circulating GDF11/8 levels are positively associated with FMD in male overweight subjects. To the best of our knowledge, our study has provided for the first time that AAV-mediated GDF11 gene transfer and systemic administration of GDF11 have a protective role against atherosclerosis progression.

It is established that GDF11 and GDF8 shared 90% protein sequence homology. Accordingly, recent studies from Egerman *et al.* and Smith *et al.* reported that key reagents that recognized

GDF11 also recognize GDF8.<sup>7,8</sup> Egerman *et al.* reported that they developed a GDF11-specific immunoassay and found a trend toward increased GDF11 levels in serum of both aged rats and humans by Western blot. However, other data showed that the increase of serum GDF11 in mice reported by Egerman *et al.* is not GDF11 but predominantly immunoglobulin light chain (the ~25 kDa band by Western blot), immunoglobulins have long been known to increase with age in C57BL/6 mice.<sup>9</sup> They also found that circulating GDF11/8 levels decline with age in multiple mammalian species. In this study, we also found circulating GDF11/8 levels decline with age in mice and in male overweight subjects. Recently, a clinical study showed that markedly reduced risk of incident heart failure hospitalization, stroke, myocardial infarction, and all-cause death in those with higher circulating GDF11/8 levels in two independent cohorts across two continents totaling 1,899 subjects with stable CHD.<sup>12</sup> In animal studies, Loffredo *et al.* demonstrated the antihypertrophic effect of GDF11 in mice by showing that administration of 0.1 mg/kg/day of GDF11 for 28 days reduced cardiac mass in aged mice.<sup>4</sup> However, Smith *et al.* argued that daily injections of biologically active rGDF11 for 28 days had no effect on overall cardiac structure and cardiac pump function in 24-month-old C57BL/6 mice.<sup>8</sup> To further characterize the antihypertrophic effect of GDF11, Loffredo *et al.* performed a dose titration study in young and aged mice and observed a

significant dose-dependent decrease of heart weight, normalized to tibia length, after only 9 days of treatment in mice receiving 0.5 or 1.0 mg/kg/day GDF11.<sup>9</sup> In this study, we found that GDF11 improved endothelial dysfunction, decreased endothelial apoptosis *in vivo* and *in vitro*, and reduced atherosclerosis plaque including the en face and cross section areas as well as enhanced mature plaque stability in apoE<sup>-/-</sup> mice. Moreover, our human study showed that circulating GDF11/8 levels are positively associated with FMD in male overweight subjects. Taken together, the data indicated that AAV-GDF11 and exogenous recombinant GDF11 can improve endothelial injury and reduce atherosclerosis lesion formation.

No significant differences on body weight, blood pressure, fasting blood glucose, and HbA1c were found among the four groups after 12 weeks of intervention, indicating that the protection of artery contributed by AAV-GDF11 and exogenous recombinant GDF11 cannot be explained by these classic cardiovascular risk factors alone. The mechanism of AAV-GDF11 and GDF11 protecting against endothelial injury and reducing atherosclerotic lesion formation in apoE<sup>-/-</sup> mice may underlie the following aspects.

A previous study reported that GDF11 treatment increased primary brain capillary endothelial cells proliferation by 22.9% as compared with controls.<sup>6</sup> Next, we questioned the effects of AAV-GDF11 and exogenous recombinant GDF11 on endothelial cell, which is crucial during atherosclerotic lesion formation.<sup>22</sup> The present animal studies demonstrated that AAV-GDF11 and exogenous recombinant GDF11 treatment alleviated the impairment of endothelium-dependent vasodilation induced by HFD, decreased the apoptosis of endothelial cells and so that preserved the endothelial cell coverage on the plaque surfaces. Consistent with the *in vivo* data, our *in vitro* experiments showed that GDF11 significantly reduced the apoptosis in PA treated MAECs. Recently, another study showed that GDF11 had no effect on proliferation and migration of human umbilical vein endothelial cell and rat aortic endothelial cells after 72 hours of treatment.<sup>28</sup> We also found GDF11 had no effect on the migration of MAECs and macrophages, however, we found GDF11 significantly promoted MAECs proliferation after 5 days of treatment, which makes endothelial cells have a certain ability to self-repair. The discrepancy may be due to different treatment time. Thus, based on these data, we can suggest that AAV-GDF11 and recombinant GDF11 could protect against endothelial injury, consequently ameliorate atherosclerosis.

Atherosclerosis is considered as an inflammatory disease and inflammatory responses mediated by inflammatory cytokines are participated and considered important in all stages of atherosclerosis.<sup>29</sup> This study showed that elevated GDF11 levels significantly reduced the mRNA expression levels of inflammatory mediators and increased antiinflammatory (IL-10) cytokines in aortas and decreased plasma inflammatory cytokines in HFD fed mice, as well as attenuated inflammatory reaction induced by PA in RAW264.7 macrophages. Therefore, the anti-inflammation of GDF11 may largely contribute to the decreased number of macrophages and T-lymphocytes in the plaque tissue and its protective effect of artery.

Previous studies found that inflammation results in insulin resistance, and the improvement of insulin sensitivity alleviates

endothelial dysfunction and atherosclerosis.<sup>30,31</sup> In this study, glucose and insulin tolerance tests in apoE<sup>-/-</sup> mice fed by HFD displayed impairment in both glucose tolerance and insulin sensitivity, and AAV-GDF11 and exogenous GDF11 treatment for 12 weeks significantly improved insulin and glucose tolerance when compared with the AAV-GFP and vehicle (refer to intraperitoneal glucose tolerance test and insulin tolerance test results), suggesting that AAV-GDF11 and recombinant GDF11 can improve insulin resistance in apoE<sup>-/-</sup> mice fed by HFD. As a result, the fasting insulin concentrations in AAV-GDF11 and recombinant GDF11 treatment groups decreased significantly. Therefore, the improvement of glucose tolerance and insulin sensitivity can partially explain the endothelium-protective as well as antiatherosclerotic effects of AAV-GDF11 and recombinant GDF11.

Pathological studies have demonstrated that not only the lesion size but also the plaque components play a key role in the development of acute coronary syndrome and arteriosclerosis.<sup>32</sup> Vulnerable plaque is characterized by increased contents of macrophages and T lymphocytes and reduced contents of collagen and VSMCs. Our data suggested that one of the key mechanisms by which AAV-GDF11 and exogenous GDF11 elicits plaque stabilization is decreasing the number of plaque-infiltrating macrophages, because macrophage lysis in advanced lesions has been involved in the generation of necrotic cores, which promote plaque instability.<sup>21,33</sup> In addition, the loss of VSMCs in the fibrous cap represents a critical mechanism in transforming stable plaque into rupture-prone lesions. This study showed that AAV-GDF11 and recombinant GDF11 treatment showed a tendency to increase the number of  $\alpha$ -SMA-positive cells in the fibrous cap within the atherosclerotic plaques in apoE<sup>-/-</sup> mice, which is relevant for plaque stability. Taken together, sustained *in vivo* expression of endogenous GDF11 or GDF11 injection not only dramatically attenuated the total extension of the plaques but also contributed to stabilize atherosclerotic plaques by selectively decreasing in macrophages and T lymphocytes and a substantial increasing in collagen and VSMCs in the aortic plaques. Moreover, macrophages in plaques may secrete proteolytic enzymes, such as MMPs, which may digest the extracellular matrix and weaken the fibrous cap.<sup>34</sup> Indeed, AAV-GDF11 and recombinant GDF11 treatment significantly inhibited MMP-2 and MMP-9 protein expression in plaques in this study. Thus, there is a possible direct link between the decreased of macrophages and MMPs and increased of collagen as well as VSMCs in these lesions, indicating that GDF11 is a powerful cytokine for altering plaque components toward a stable plaque phenotype.

Next, we questioned the molecular signal pathways for the protective effect of GDF11 on artery. It is well known that GDF11 exerts its function by interacting with activin type IIA and IIB receptors<sup>2</sup> and type I receptor Alk5 (ref. 3) to induce canonical Smad signaling pathway. This study showed that AAV-GDF11 and exogenous GDF11 activated phosphorylation of Smad 2/3 in aortas of apoE<sup>-/-</sup> mice and consequently induced less plaques compared with the AAV-GFP and vehicle. The *in vitro* experiments showed that GDF11 enhanced the phosphorylation of Smad 2/3 in MAECs and RAW 264.7 macrophages, and the antiapoptotic effects of GDF11 could be attenuated by the Smad3 inhibitor. In addition, TGF- $\beta$  and BMP receptor activation results in activation

of several other non-Smad signaling pathways in a context-dependent manner. Non-Smad signaling pathways can involve the ERK1/2, JNK, and the Akt pathway, and these can crosstalk with the Smad pathways.<sup>35</sup> This study showed that GDF11 improved endothelial dysfunction by increasing the phosphorylation of AMPK and eNOS and consequently increased serum NO concentrations in apoE<sup>-/-</sup> mice. Consistent with the animal experiments, GDF11 increased the phosphorylation of AMPK and eNOS, and production of NO in cultured MAECs, whereas the specific inhibitor of AMPK or eNOS, such as Compound C or L-NAME, attenuates these effects of GDF11. Furthermore, pretreatment with L-NAME significantly attenuated the inhibitory effects of GDF11 on endothelial apoptosis. Of note, previous studies suggested that the control of dysregulated mitogen-activated protein kinase cascade and NF- $\kappa$ B activation could be a potential target in the treatment of atherosclerosis.<sup>36,37</sup> This study further showed that GDF11 significantly inhibited PA-induced activation of JNK and NF- $\kappa$ B and consequently inhibited the inflammatory cytokines expression in RAW264.7 macrophages. Overall, our data suggest that GDF11 protects artery through the canonical (Smad2/3) and non-canonical (AMPK/eNOS, JNK, and NF- $\kappa$ B) signaling pathways.

Due to the low toxicity and efficient and long-term transduction *in vivo*, AAV vectors are currently evaluated in many animals and clinical studies.<sup>38,39</sup> Intriguingly, AAV vector genome realized liver transduction and subsequent released into the circulation, which is the most likely mechanism. This study demonstrates successful *in vivo* transduction via AAV2 vector which facilitated sustained GDF11 overexpression and obtained similar results on antiatherosclerotic effect compared with repeated intraperitoneal injection of recombinant GDF11, strongly suggesting that AAV represents a potential alternative to recombinant protein injection.

Some limitations should be mentioned here. Firstly, myostatin (GDF8) is a close structural homologue of GDF11, with 90% amino acid sequence identity shared in their mature active-forms.<sup>40</sup> Thus, our assay for mouse and human serum GDF11 does not distinguish circulating GDF11 and GDF8. As a result, we did not accurately determine the changes of GDF11 in mice and in human. Secondly, since alterations of circulating monocytes and lymphocytes might affect atherosclerotic plaque formation directly. However, in this study, we did not measure the circulating cells in mice, such we cannot evaluate the changes of circulating cells before and after GDF11 intervention. Thirdly, we did not explore the Akt/mammalian target of rapamycin (mTOR) pathway, because some studies showed that Akt/mTOR pathway was involved in cardiovascular diseases.<sup>41</sup> Fourthly, the number of study subjects in human is relatively small. It is difficult to exclude bias in the results, which should be confirmed in large studies.

In conclusion, AAV-GDF11 and recombinant GDF11 alleviated atherosclerotic lesions formation via protecting against endothelial injury, decreasing plaque-infiltrating inflammatory cells and alleviating inflammation reactions. The signal mechanisms underlying these effects may involve the canonical (TGF- $\beta$ /Smad) and noncanonical (AMPK/eNOS, JNK, and NF- $\kappa$ B) signaling pathways. Thus, AAV-GDF11 or recombinant GDF11 may open a new therapeutic strategy for treating atherosclerosis.

## MATERIALS AND METHODS

**AAV-GDF11 construct.** The GDF11 cDNA (GenBank accession number NM\_010272.1) was obtained by reverse transcriptase-polymerase chain reaction amplification. The GDF11 cDNA was inserted into the AAV2 vector plasmid pSNAV1 under the control of the constitutive cytomegalovirus promoter to construct pSNAV1/GDF11. The pSNAV1/GDF11 was transfected into 293 T-cells and large-scale rAAV production and purification were described previously.<sup>42</sup> Viral preparations used for animal transduction had titers between  $1 \times 10^{12}$  and  $1 \times 10^{13}$  viral genome particles per 1 ml.

**Animals.** The experiments conformed to the National Institutes of Health Guidelines for the Use of Laboratory Animals. All animal experimental protocols were approved by the animal ethics committee of the Wuhan General Hospital of Guangzhou Command. One hundred and two male 4-week-old apoE<sup>-/-</sup> mice (The Jackson Laboratory, Bar Harbor, ME) were housed in a specific-pathogen-free environment with a 12-hour light/dark cycle, and unrestricted access to water. Of those mice 25 were selected randomly as normal chow control group, fed with normal chow from 4-week-old to the end of the study, the rest of those mice were fed with a HFD (45% kcal fat, 35% kcal carbohydrates, and 20% kcal protein) from 4-week-old to the end of the study. Of those, 25 mice fed with HFD were selected randomly as HFD control group. The HFD control group and the normal chow control group were just for the evaluation of weight, FFA and serum GDF11/8 at different time points (-8, 0, 4, 8, and 12 weeks) (see **Supplementary Figure S1b-d**) and 5 mice were killed at each time point.

After 8 weeks of HFD, the rest 52 mice were randomly divided into four groups: AAV-GDF11 and AAV-GFP treatment groups (received a single injection of 250  $\mu$ l purified AAV-GDF11 or 250  $\mu$ l AAV-GFP through the tail vein), vehicle and recombinant GDF11 treatment groups (received a daily intraperitoneal administration of pH = 3, 250  $\mu$ l citrate buffer or 250  $\mu$ l citrate buffer containing GDF11 (0.1 mg/kg, PeproTech, Rocky Hill, NJ)).<sup>4</sup> After 4 weeks of treatment, three mice from each group were anesthetized by an intraperitoneal injection of pentobarbital sodium (60 mg/kg body weight) and killed for the measurements of endothelial function and serum GDF11/8 in all groups and the GDF11 expression of livers and aortas in AAV-GDF11 and AAV-GFP groups. After 12 weeks of treatment, the rest of animals ( $n = 10$  mice in each group) were anesthetized by the same way and killed for blood tests and histological examination.

**Glucose and insulin tolerance test.** Intraperitoneal glucose tolerance test and insulin tolerance test were performed before 1 day and 12 weeks after different interventions in 4 groups ( $n = 13$  mice before treatment and  $n = 10$  mice after treatment) according to our previous report.<sup>43</sup>

**Endothelial function assessment.** The thoracic aortas were harvested under the stereo-microscope (Olympus, Tokyo, Japan) and cut into 4 mm rings with special care to preserve the endothelium. The endothelium-dependent and endothelium-independent vasodilation responses were measured according to our previous report.<sup>43</sup>

**Atherosclerosis analysis and immunohistochemistry.** To evaluate the atherosclerotic lesions, two complementary approaches (en face whole and histological section analyses) were performed according to our previous report.<sup>43</sup> After treatment for 12 weeks, whole aorta extending from the ascending aorta to the abdominal bifurcation was opened longitudinally and stained with Oil-red-O (Sigma-Aldrich, St.Louis, MO) to analyze the en face atherosclerotic lesions area ( $n = 4$  mice in each group). To quantify luminal cross-sectional area involved by atherosclerotic plaque, 10 sections obtained every 20  $\mu$ m from the aortic arch ( $n = 4$  mice in each group) were stained with hematoxylin and eosin. For detection of targeted protein expression levels in all groups, the immunohistochemical analysis was used in serial plaque sections from the aortic arch ( $n = 4$  mice in each group). The immunohistochemistry assays for CD68, CD90,  $\alpha$ -smooth muscle actin, MMP-2 and MMP-9 were shown in online **Supplementary Information**.

**Analysis of apoptosis in vivo.** According to our previous report,<sup>43</sup> endothelial cell apoptosis in thoracic aortas was detected by double stain with terminal deoxynucleotidyl transferase-mediated dUTP-biotin nick end labeling and anti-CD31. Electron microscopy was performed on thoracic segments using ultrathin sections and examined with a Nikon EclipseE800 light microscope (Nikon, Tokyo, Japan).

**Cell cultures.** MAECs for *in vitro* experiments were isolated from aortas of apoE<sup>-/-</sup> mice (6–8 weeks of age) as described.<sup>44</sup> RAW264.7 cells were purchased from the Cell Bank of the Chinese Academy of Sciences (Shanghai, China). The details for cell cultures were available in online **Supplementary Information**.

**Cell signaling analysis.** For pSMAD assays, MAECs and RAW264.7 cells were divided into three treatment groups: vehicle-treated group, GDF11-treated group (50 ng/ml) and GDF11 + SB431542 (10 μmol/l). Cells were pretreated with SB431542 for 30 minutes, and then treated with GDF11 for 30 minutes. For P-eNOS assays, MAECs were divided into five groups and pretreated with inhibitors against AMPK (Compound C, 500 μmol/l, Compound C group) or eNOS (L-NAME, 500 μmol/l, L-NAME group) or both of them for 30 minutes before GDF11 (50 ng/ml) was added. After cultured for 30 minutes, the protein expression levels of P-AMPK, AMPK, P-eNOS, eNOS, P-PKA, PKA, P-Akt, and Akt were assessed by Western blot.

**Inflammatory analysis.** RAW264.7 cells were divided into four groups: vehicle-treated group, PA-treated group, PA + GDF11-treated group (50 ng/ml), and PA + GDF11 + SB431542 (10 μmol/l) group. Cells were pretreated with TβR1 inhibitor for 30 minutes, and then treated with GDF11 for 1 hour followed by stimulation with PA (0.4 mmol/l). After treatment for 30 minutes, the protein expression levels of P-ERK1/2, ERK1/2, P-JNK, JNK, and NF-κB p65 nuclear translocation were assessed by Western blot. After the same treatment for 16 hours, culture media levels of IL-6, TNF-α, and MCP-1 were determined using enzyme-linked immunosorbent assay according to the manufacturer's instructions (R&D Systems, Minneapolis, MN).

**The assessments of other parameters.** The Body weight, blood pressure and blood biochemical analysis, glucose and insulin tolerance test for mouse, apoptosis analysis, immunohistochemistry, NO measurement, real time polymerase chain reaction, Western blot analysis, proliferation and migration analysis *in vitro* are described in online **Supplementary Information**.

#### Human studies

**Subjects.** From July 2014 to July 2015, a total of 140 successive newly diagnosed Chinese male overweight subjects from Wuhan area (aged 30–65 years, mean 48.2 ± 9.5), who referred to our hospital for health examination, were selected randomly in this study. Overweight subjects were defined as body mass index ≥ 25, and <30 kg/m<sup>2</sup> (WHO criteria). The details for inclusion and exclusion criteria were shown in online **Supplementary Information**.

**Biochemical measurements.** Blood samples were obtained from participants after a 12-hour fast. Aliquots of serum and plasma were stored at -80°C and were not thawed until analyzed. Serum GDF11/8 concentrations were measured in duplicate by using the enzyme-linked immunosorbent assay kits (Elabscience, Wuhan, China), in accordance with the manufacturer's instructions. The sensitivity of the assay was 9.375 pg/ml and the linear range of the standard was 15.625–1,000 pg/ml. The intra- and interassay coefficients of variation were <10%. The details for other biochemical parameters were shown in online **Supplementary Information**.

**Ultrasound study of the brachial artery.** The vascular studies of the brachial artery were performed noninvasively in the AM following a controlled diet, as described in our previous publications.<sup>45,46</sup>

**Statistical analysis.** Data are expressed as mean ± SD. Differences between two groups were tested with unpaired Student's *t*-test. Data of multiple groups were compared using one-way analysis of variance followed by least significant difference *t*-test. A *P*-value < 0.05 was considered statistically significant. All analyses were performed with SPSS 21.0 (IBM, Somers, NY). The statistical methods for human study were shown in online **Supplementary Information**.

#### SUPPLEMENTARY MATERIAL

**Figure S1.** GDF11 influenced the body weight, serum free fatty acids and GDF11/8 levels in mice fed with normal chow or high-fat diet.

**Figure S2.** AAV-GDF11 and GDF11 improved glucose tolerance in apoE<sup>-/-</sup> mice.

**Figure S3.** GDF11 improved insulin tolerance in apoE<sup>-/-</sup> mice.

**Figure S4.** AAV-GDF11 and GDF11 reduced matrix metalloproteinase-2 (MMP-2) and MMP-9 protein expression in plaques.

**Figure S5.** GDF11 induced the proliferation of MAECs but had no effect on the migration of MAECs and macrophages.

**Figure S6.** Identification of the optimum incubation condition in cell experiments.

**Figure S7.** GDF11 reduced palmitic acid (PA)-induced inflammatory cytokines expression in RAW264.7 macrophages.

**Figure S8.** GDF11 promoted nitric oxide (NO) production *in vivo* and *in vitro*.

**Figure S9.** GDF11 activated AMPK-eNOS signaling in cultured MAECs.

**Table S1.** Body weight and blood pressure levels at 0 week and 12 week of the experiments in apoE<sup>-/-</sup> mice.

**Table S2.** The metabolic characteristics at the end of the experiments in apoE<sup>-/-</sup> mice.

**Table S3.** Clinical and biochemical characteristics in control and in overweight subjects.

**Table S4.** Clinical and biochemical characteristics in overweight subjects according to the quartiles of FMD levels.

**Table S5.** Multiple stepwise regression analysis (forward) with FMD level as dependent variable.

**Table S6.** The odds ratio for the lower FMD levels according to GDF11/8 levels.

#### Supplementary Information

#### ACKNOWLEDGMENTS

This work was supported by National Natural Science Foundation of China (number 81370896 and number 81570730). Guangda Xiang performed the research design and the clinical experiment; Wen Mei conducted the animal experiment; Yixiang Li, Huan Li, Min Liu, and Lin Xiang performed the *in vitro* experiment; Lingwei Xiang conducted data analysis; Junyan Lu and Jing Dong conducted the manuscript writing. The authors declare no competing financial interests.

#### REFERENCES

- Gamer, LW, Wolfman, NM, Celeste, AJ, Hattersley, G, Hewick, R and Rosen, V (1999). A novel BMP expressed in developing mouse limb, spinal cord, and tail bud is a potent mesoderm inducer in *Xenopus* embryos. *Dev Biol* **208**: 222–232.
- Oh, SP, Yeo, CY, Lee, Y, Schrewe, H, Whitman, M and Li, E (2002). Activin type IIA and IIB receptors mediate Gdf11 signaling in axial vertebral patterning. *Genes Dev* **16**: 2749–2754.
- Andersson, O, Reissmann, E and Ibáñez, CF (2006). Growth differentiation factor 11 signals through the transforming growth factor-beta receptor ALK5 to regionalize the anterior-posterior axis. *EMBO Rep* **7**: 831–837.
- Loffredo, FS, Steinhauser, ML, Jay, SM, Gannon, J, Pancoast, JR, Yalamanchi, P *et al.* (2013). Growth differentiation factor 11 is a circulating factor that reverses age-related cardiac hypertrophy. *Cell* **153**: 828–839.
- Sinha, M, Jang, YC, Oh, J, Khong, D, Wu, EY, Manohar, R *et al.* (2014). Restoring systemic GDF11 levels reverses age-related dysfunction in mouse skeletal muscle. *Science* **344**: 649–652.
- Katsimpardi, L, Litterman, NK, Schein, PA, Miller, CM, Loffredo, FS, Wojtkiewicz, GR *et al.* (2014). Vascular and neurogenic rejuvenation of the aging mouse brain by young systemic factors. *Science* **344**: 630–634.
- Egerman, MA, Cadena, SM, Gilbert, JA, Meyer, A, Nelson, HN, Swalley, SE *et al.* (2015). GDF11 increases with age and inhibits skeletal muscle regeneration. *Cell Metab* **22**: 164–174.
- Smith, SC, Zhang, X, Zhang, X, Gross, P, Starosta, T, Mohsin, S *et al.* (2015). GDF11 does not rescue aging-related pathological hypertrophy. *Circ Res* **117**: 926–932.

9. Poggolini, T, Vujic, A, Yang, P, Macias-Trevino, C, Uygur, A, Loffredo, FS *et al.* (2016). Circulating growth differentiation factor 11/8 levels decline with age. *Circ Res* **118**: 29–37.
10. Fadini, GP, Menegazzo, L, Bonora, BM, Mazzucato, M, Persano, S, Vigili de Kreutzenberg, S *et al.* (2015). Effects of age, diabetes, and vascular disease on growth differentiation factor 11: first-in-human study. *Diabetes Care* **38**: e118–e119.
11. Heidecker, B, Olson, K, Beatty, A (2015). Low levels of growth differentiation factor 11 and high levels of its inhibitor follistatin-like 3 are associated with adverse cardiovascular outcomes in humans. *J Am Coll Cardiol* **65**: A999.
12. Olson, KA, Beatty, AL, Heidecker, B, Regan, MC, Brody, EN, Foreman, T *et al.* (2015). Association of growth differentiation factor 11/8, putative anti-ageing factor, with cardiovascular outcomes and overall mortality in humans: analysis of the heart and soul and HUNT3 cohorts. *Eur Heart J* **36**: 3426–3434.
13. Zhang, L, Connelly, JJ, Peppel, K, Brian, L, Shah, SH, Nelson, S *et al.* (2010). Aging-related atherosclerosis is exacerbated by arterial expression of tumor necrosis factor receptor-1: evidence from mouse models and human association studies. *Hum Mol Genet* **19**: 2754–2766.
14. Mattace-Raso, F, van Popele, NM, Schalekamp, MA and van der Cammen, TJ (2002). Intima-media thickness of the common carotid arteries is related to coronary atherosclerosis and left ventricular hypertrophy in older adults. *Angiology* **53**: 569–574.
15. Bos, D, van der Rijk, MJ, Geeraedts, TE, Hofman, A, Krestin, GP, Witteman, JC *et al.* (2012). Intracranial carotid artery atherosclerosis: prevalence and risk factors in the general population. *Stroke* **43**: 1878–1884.
16. Jalkanen, J, Leppänen, P, Pajusola, K, Näränen, O, Mähönen, A, Vähäkangas, E *et al.* (2003). Adeno-associated virus-mediated gene transfer of a secreted decoy human macrophage scavenger receptor reduces atherosclerotic lesion formation in LDL receptor knockout mice. *Mol Ther* **8**: 903–910.
17. Finkenzeller, G, Stark, GB and Strassburg, S (2015). Growth differentiation factor 11 supports migration and sprouting of endothelial progenitor cells. *J Surg Res* **198**: 50–56.
18. Birck, MM, Saraste, A, Hyttel, P, Odermarsky, M, Liuba, P, Saukko, P *et al.* (2013). Endothelial cell death and intimal foam cell accumulation in the coronary artery of infected hypercholesterolemic minipigs. *J Cardiovasc Transl Res* **6**: 579–587.
19. Bonetti, PO, Lerman, LO and Lerman, A (2003). Endothelial dysfunction: a marker of atherosclerotic risk. *Arterioscler Thromb Vasc Biol* **23**: 168–175.
20. Galis, ZS and Khatri, JJ (2002). Matrix metalloproteinases in vascular remodeling and atherogenesis: the good, the bad, and the ugly. *Circ Res* **90**: 251–262.
21. Libby, P (2002). Inflammation in atherosclerosis. *Nature* **420**: 868–874.
22. Tripathy, D, Mohanty, P, Dhindsa, S, Syed, T, Ghanim, H, Aljada, A *et al.* (2003). Elevation of free fatty acids induces inflammation and impairs vascular reactivity in healthy subjects. *Diabetes* **52**: 2882–2887.
23. Hansson, GK, Libby, P, Schönbeck, U and Yan, ZQ (2002). Innate and adaptive immunity in the pathogenesis of atherosclerosis. *Circ Res* **91**: 281–291.
24. Matsubara, J, Sugiyama, S, Sugamura, K, Nakamura, T, Fujiwara, Y, Akiyama, E *et al.* (2012). A dipeptidyl peptidase-4 inhibitor, des-fluoro-sitagliptin, improves endothelial function and reduces atherosclerotic lesion formation in apolipoprotein E-deficient mice. *J Am Coll Cardiol* **59**: 265–276.
25. Moncada, S, Palmer, RM and Higgs, EA (1991). Nitric oxide: physiology, pathophysiology, and pharmacology. *Pharmacol Rev* **43**: 109–142.
26. Oemar, BS, Tschudi, MR, Godoy, N, Brovkovich, V, Malinski, T and Lüscher, TF (1998). Reduced endothelial nitric oxide synthase expression and production in human atherosclerosis. *Circulation* **97**: 2494–2498.
27. Michell, BJ, Chen Zp, Tiganis, T, Stapleton, D, Katsis, F, Power, DA *et al.* (2001). Coordinated control of endothelial nitric-oxide synthase phosphorylation by protein kinase C and the cAMP-dependent protein kinase. *J Biol Chem* **276**: 17625–17628.
28. Zhang, YH, Cheng, F, Du, XT, Gao, JL, Xiao, XL, Li, N *et al.* (2016). GDF11/BMP11 activates both smad1/5/8 and smad2/3 signals but shows no significant effect on proliferation and migration of human umbilical vein endothelial cells. *Oncotarget* **7**: 12063–12074.
29. Tuttolomondo, A (2012). Editorial: treatment of atherosclerosis as an inflammatory disease. *Curr Pharm Des* **18**: 4265.
30. Arcaro, G, Cretti, A, Balzano, S, Lechi, A, Muggeo, M, Bonora, E *et al.* (2002). Insulin causes endothelial dysfunction in humans: sites and mechanisms. *Circulation* **105**: 576–582.
31. Lteif, AA, Han, K and Mather, KJ (2005). Obesity, insulin resistance, and the metabolic syndrome: determinants of endothelial dysfunction in whites and blacks. *Circulation* **112**: 32–38.
32. Shiomi, M, Ito, T, Hirouchi, Y and Enomoto, M (2001). Fibromuscular cap composition is important for the stability of established atherosclerotic plaques in mature WHHL rabbits treated with statins. *Atherosclerosis* **157**: 75–84.
33. Glass, CK, Witztum, JL (2001). Atherosclerosis: the road ahead. *Cell* **104**: 503–516.
34. Gough, PJ, Gomez, IG, Wille, PT and Raines, EW (2006). Macrophage expression of active MMP-9 induces acute plaque disruption in apoE-deficient mice. *J Clin Invest* **116**: 59–69.
35. Guo, X and Wang, XF (2009). Signaling cross-talk between TGF-beta/BMP and other pathways. *Cell Res* **19**: 71–88.
36. Senokuchi, T, Matsumura, T, Matsuo, T, Yano, M, Nishikawa, T, Araki, E. (2003). 4P-0977 Extracellular signal-regulated kinase and p38 mitogen-activated protein kinases are involved in oxidized low density lipoprotein-induced macrophage proliferation. *Atherosclerosis Supp* **4**: 289.
37. Chang, L and Karin, M (2001). Mammalian MAP kinase signalling cascades. *Nature* **410**: 37–40.
38. Yin, K, Tang, SL, Yu, XH, Tu, GH, He, RF, Li, JF *et al.* (2013). Apolipoprotein A-I inhibits LPS-induced atherosclerosis in ApoE(-/-) mice possibly via activated STAT3-mediated upregulation of tristetraprolin. *Acta Pharmacol Sin* **34**: 837–846.
39. Warrington, KH Jr and Herzog, RW (2006). Treatment of human disease by adeno-associated viral gene transfer. *Hum Genet* **119**: 571–603.
40. Nakashima, M, Toyono, T, Akamine, A and Joyner, A (1999). Expression of growth/differentiation factor 11, a new member of the BMP/TGFbeta superfamily during mouse embryogenesis. *Mech Dev* **80**: 185–189.
41. Santulli, G and Totary-Jain, H (2013). Tailoring mTOR-based therapy: molecular evidence and clinical challenges. *Pharmacogenomics* **14**: 1517–1526.
42. Wu, X, Dong, X, Wu, Z, Cao, H, Niu, D, Qu, J *et al.* (2001). A novel method for purification of recombinant adeno-associated virus vectors on a large scale. *Chinese Sci Bull* **46**: 485–488.
43. Lu, J, Xiang, G, Liu, M, Mei, W, Xiang, L and Dong, J (2015). Irisin protects against endothelial injury and ameliorates atherosclerosis in apolipoprotein E-Null diabetic mice. *Atherosclerosis* **243**: 438–448.
44. Kobayashi, M, Inoue, K, Warabi, E, Minami, T and Kodama, T (2005). A simple method of isolating mouse aortic endothelial cells. *J Atheroscler Thromb* **12**: 138–142.
45. Xiang, GD, Xu, L, Zhao, LS, Yue, L and Hou, J (2006). The relationship between plasma osteoprotegerin and endothelium-dependent arterial dilation in type 2 diabetes. *Diabetes* **55**: 2126–2131.
46. Guangda, X and Yuhua, W (2003). Apolipoprotein e4 allele and endothelium-dependent arterial dilation in type 2 diabetes mellitus without angiopathy. *Diabetologia* **46**: 514–519.